

# SEAMLESS 1.3 GHz COPPER CAVITIES FOR Nb COATINGS: COLD TEST RESULTS OF TWO DIFFERENT APPROACHES\*

L. Vega Cid <sup>†</sup>, S. Atieh, L.M.A. Ferreira, L. Laín-Amador, S.B. Leith, C. Pereira, G.J. Rosaz, K. Scibor, W. Venturini Delsolaro, P. Vidal García <sup>‡1</sup>, CERN, 1211 Geneva, Switzerland  
<sup>1</sup>also at CIEMAT, 28040 Madrid, Spain

## Abstract

A necessary condition for high SRF performances in thin film coated cavities is the absence of substrate defects. For instance, in the past, defects originated around electron beam welds in high magnetic field areas have been shown to be the cause of performance limitations in Nb/Cu cavities. Seamless cavities are therefore good candidates to allow an optimization of the coating parameters without the pitfalls of a changing substrate. In this work, we present the first results of two different methods to produce seamless cavities applied to 1.3 GHz copper single cells coated with thin Nb films by means of HIPIMS. A first method consists in electroplating the copper resonator on precisely machined aluminum mandrels, which are then dissolved chemically. As an alternative and a cross check, one cavity was machined directly from the bulk. Both cavities were coated with HIPIMS Nb films using the same coating parameters and the SRF performance was measured down to 1.8 K with a variable coupler to minimize the measurement uncertainty.

## INTRODUCTION

The thin film technology has been historically used for superconducting radio frequency cavities at CERN, where various accelerators use SRF cavities made of Nb coatings on copper substrates. It was first implemented in the LEP [1], and later in the LHC and HIE-ISOLDE [2]. It is also expected to be one of the selected technologies for the future circular colliders (FCC) [3]. Coated cavities have several advantageous features. On one hand, raw material costs are lower. Also, cryogenics costs are reduced thanks to the higher thermal diffusivity of copper and optimized BCS surface resistance of sputtered Nb [4], allowing operation in liquid helium bath at 4.2 K instead of superfluid helium. Moreover, copper substrates provide sufficient thermal and mechanical stability so that thermal breakdowns do not occur and microphonics can be fully suppressed. Nb on copper cavities are also less sensitive to magnetic flux trapping, allowing savings on magnetic shielding of cryomodules [5].

However, degradation of the RF performance at high fields has been historically observed in these cavities [6]. The nature of this phenomenon, known as Q slope, has been the subject of research and is not yet fully explained. In any case, the presence of defects in the copper substrate is a known cause of performance degradation. The influence of

the substrate on the growth process of thin films, and how it is affected by the microstructure of the copper is reported in [7]. To mitigate this, efforts have to be made on improving the quality of the thin film cavities at all levels:

- Interface between Nb film and substrate: a good adhesion is key to avoid the occurrence of peel-offs. A significant thermal resistance in the bad contact region can lead to a local increase of the temperature, and consequently of the BCS surface resistance, leading to the observed Q-drop [8].
- Quality of the film: an extensive R&D campaign has been carried out at CERN for finding and optimizing the best thin film deposition technique [9]. High Impulse Power Magnetron Sputtering (HIPIMS) has given promising results from the RF point of view, allowing for a dense, void-free layer at all the impinging angles of the niobium coating flux [10, 11]. In this work, the cavities under study have been coated with this optimized method.
- Quality of the substrate: defects in the substrate are propagated to the thin film deposited on top. This became evident after the experience with the HIE-ISOLDE quarter wave resonator (QWR), where a systematic loss of performance was observed in the series of cavities manufactured with electron beam welding. This was correlated with the presence of microscopic cracks in the welded region [12], and it served as motivation for producing a seamless substrate machined from a copper billet [13]. Dedicated experiments revealed that by controlling environmental variables (magnetic shielding and cool down dynamics [14]), Nb films deposited on these seamless substrates showed record-breaking RF performances for the Nb/Cu technology [15]. Following these studies, in this paper we investigate the performance of two 1.3 GHz Nb/Cu cavities produced with seamless copper substrates by two different methods.

## PRODUCTION OF THE SUBSTRATES

In view of the importance of avoiding welds on high RF field regions, finding a technique for producing seamless substrates for mass production of SRF cavities becomes a keystone. Not only it has to be feasible in terms of costs and manufacturing time, but the quality has to be reproducible in a large scale production. Several methods have been already investigated, such as spinning [16] or hydroforming [17]. The disadvantage of those techniques is the varying wall thickness along the profile and extensive damage to the over strained material [18]. Regarding the hydroforming, a major issue was a higher intrinsic content in hydrogen resulting

\* C. Pereira acknowledges the financial support provided by the Fundação para a Ciência e Tecnologia, project SFRH/BEST/150601/2020

<sup>†</sup> lorena.vega@cern.ch

<sup>‡</sup> pablo.vidal.garcia@cern.ch

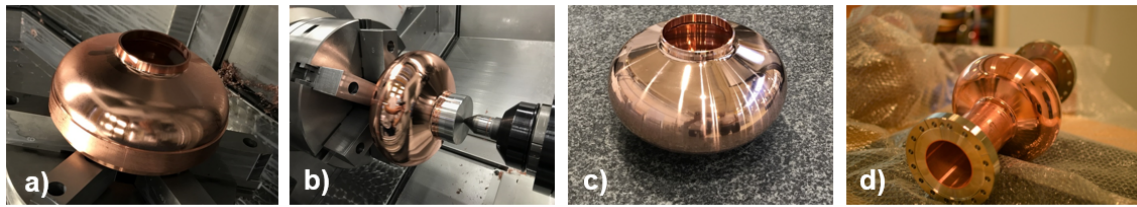


Figure 1: Process for manufacturing the copper seamless substrate by machining from a bulk copper billet: a) First half cell machined. b) Second half cell machined. c) Machined cell. d) Cell e-beam welded to cut-offs.

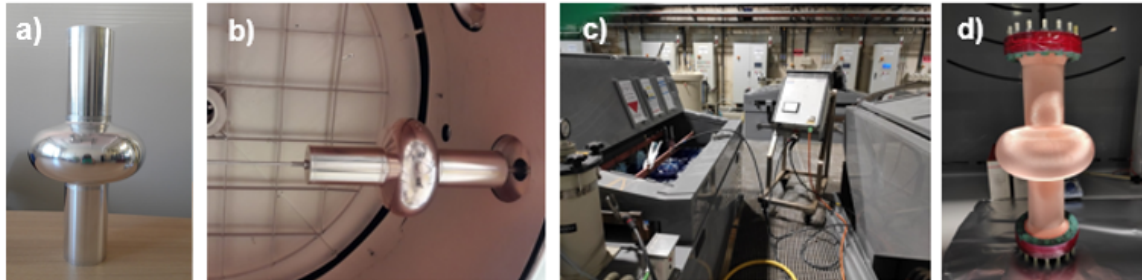


Figure 2: Process for manufacturing the copper seamless substrate by electroforming: a) Preparation of the aluminium mandrel. b) Deposition of Cu thin film by PVD. c) Copper electroforming and mandrel removal. d) Final assembly.

systematically in poorer performance. Regarding the spinning, it has never been capable of producing machine grade mechanical tolerances. At CERN, two seamless copper substrates of 1.3 GHz cavities have been recently produced: one has been manufactured by means of electroforming, named L1, to investigate the feasibility of using this technique for mass production. The other one, named BM1, has been machined from a copper block to serve as benchmarking.

The steps to produce the cavity machined from the bulk copper billet include turning roughing, 5-axis milling roughing, and turning finishing of inner and external shape [18]. Once the cell was manufactured, it was e-beam welded to the cut-offs (see Fig. 1).

Regarding the copper electroforming, this technique was already developed and applied at CERN [19]. The feasibility of applying it to produce seamless copper substrates for 1.3 GHz cavities has been demonstrated [20,21]. The main steps of the process are the preparation of the aluminium mandrel and flanges, the copper metallization of the mandrel by performing a thin film layer by physical vapour deposition, the copper electroforming step where the flanges are incorporated to the cavity and the removal of the mandrel by chemical dissolution. They are represented in Fig. 2 [20].

## METHODOLOGY

The RF performance was measured by standard methods in a small vertical cryostat at the CERN Cryolab following the algorithms described in [22]. The main observable was the unloaded quality factor  $Q_0$  as a function of the accelerating field  $E_{acc}$ . For each data point taken in CW, the reflected power was minimized to reduce the measurement uncertainty. This was achieved by means of a mobile input coupler which was controlled to maintain critical coupling during the measurements.

First, a measurement of the  $Q_0$  as a function of the accelerating field  $E_{acc}$  is carried out by sweeping the input power while maintaining constant the temperature of the helium bath. This is done at 4.2 K, and also at 1.85 K.

Another measurement is performed to obtain the  $Q_0$  as a function of temperature, while keeping a fixed accelerating field and adjusting the input coupler to maintain critical coupling. The average surface resistance, extracted from dividing the geometrical factor  $G$  by the measured  $Q_0$ , was analysed with the conventional formula:

$$R_s = R_{res} + \frac{A_{BCS}}{T} e^{-\frac{\Delta(0)}{k_B T}}; \quad (1)$$

being  $R_{res}$  the residual resistance and the second term is the BCS contribution, where  $A_{BCS}$  is a parameter that depends on the purity of the material and  $\Delta(0)$  is the superconducting energy gap at  $T = 0$  K. Another scan is done to measure the shift in the resonance frequency when increasing the temperature towards the superconducting to normal transition. The change in the resonance frequency  $\Delta f$  is related to the change in the penetration depth  $\Delta\lambda$  by using Slater's Theorem. Then, this is fitted as a function of the temperature:

$$\lambda = \frac{\lambda(0)}{\sqrt{1 - \left(\frac{T}{T_c}\right)^4}} + c, \quad (2)$$

where  $\lambda(0)$  is the penetration depth at 0 K,  $T_c$  is the critical temperature, and  $c$  is the offset to obtain the measured  $\lambda$ .

## RESULTS

### Substrate BM1

After machining, the cavity substrate BM1 was degreased and a sulfo-chromic acid rinsing was applied for passivation, followed by a high pressure water rinsing (HPWR) at 100 bar. Then, the Nb coating was directly applied without prior

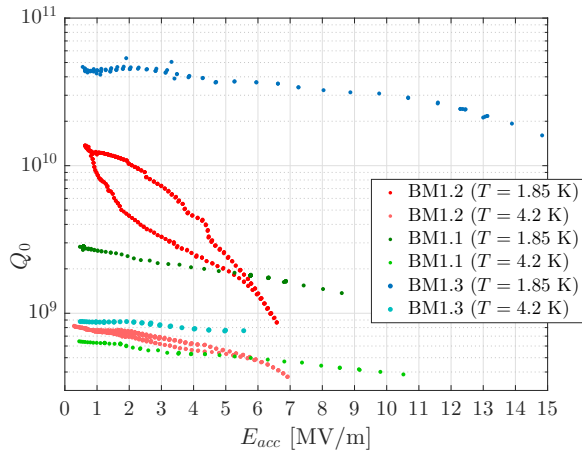


Figure 3: Quality factor ( $Q_0$ ) vs accelerating field ( $E_{acc}$ ) of the tested BM1 coatings at normal and superfluid LHe.

Table 1: SRF Parameters of Tested BM1 Coatings

	BM1.1	BM1.2	BM1.3
$R_{res}$	95.63 n $\Omega$	19.99 n $\Omega$	4.4 n $\Omega$
$\lambda(0)$	53.96 nm	51.73 nm	49.82 nm
$T_c$	9.317 K	9.312 K	9.321 K
$A_{BCS}$	1.68e5 n $\Omega$ ·K	1.56e5 n $\Omega$ ·K	1.44e5 n $\Omega$ ·K
$\Delta(0)/k_B$	20.19 K	20.11 K	20.27 K

Table 2: SRF Parameters of BM1.2 for Different Thermal Cycles

	Test #1	Test #2	Test #3
$B_{ex,0}$	12.9 $\mu$ T	4.7 $\mu$ T	7.6 $\mu$ T
$R_{res}$	31.03 n $\Omega$	19.99 n $\Omega$	23.39 n $\Omega$
$\lambda(0)$	53.17 nm	51.73 nm	49.54 nm
$T_c$	9.321	9.312 K	9.313
$A_{BCS}$	1.58e5 n $\Omega$ ·K	1.56e5 n $\Omega$ ·K	1.44e5 n $\Omega$ ·K
$\Delta(0)/k_B$	19.89 K	20.11 K	19.89 K

chemical polishing via HiPIMS deposition according to the parameters reported in Table 3.

Table 3: HiPIMS Parameters Used for Cavities Coating

HiPIMS coating parameters	
frequency	100 Hz
pulse duration	200 $\mu$ s
average power	1.2 kW
bias voltage	-75V
sputtering gas	Kr
sputtering pressure	2.3 $10^{-3}$ mbar
coating temperature	150 $^{\circ}$ C
coating duration	6hours

The cavity was prepared for RF test with a HPWR at 50 bar. This first coating was named BM1.1. Note that as a consequence of the machining, a damaged layer of 1 to 2  $\mu$ m was produced at the surface. No additional treatment was applied, aiming at quantifying the impact of an as machined surface state upon the RF performance.

In Fig. 3  $Q_0$ -curves as function of  $E_{acc}$  are represented for the first three coatings applied on the BM1 substrate, BM1.1, BM1.2 and BM1.3, measured at  $T = 4.2$  K and at  $T = 1.85$  K. All tests were terminated by administrative limits, which impose a zero threshold on the radiation interlock at the CERN cryolab. As it can be seen, the Q-slope in BM1.1 was mitigated up to  $E_{acc} \approx 8.5 - 10.5$  MV/m, both at 1.85 K and 4.2 K, but the residual resistance was high. The complete set of fitted parameters is given in Table 1. The coating was stripped and a 20min SUBU [23] was performed to start removing the damaged layer before applying again the Nb coating. This second coating was named BM1.2.

As it can be appreciated in Fig. 3 there is a striking difference in RF behaviour between BM1.1 and BM1.2, which only differed for the removal of a fraction of the surface damaged layer prior to coating. Indeed, the residual resistance was reduced by a factor of  $\approx 4.7$  (see Table 1). However, the Q slope at 1.85 K was more significant in this case.

Given the improved value of residual resistance at very low field, the test was repeated by performing thermal cycles consisting of passing the transition from normal to superconducting regime at different cooling rates. It has to be noted that there is no way to control accurately the cooling rate in the available measurement setup. Recorded data from a flux gate installed in a vertical position at the cut-off just above the cell give an idea of the magnetic flux expelled in the different thermal cycles. For each cycle, the fitted parameters were extracted from the scans ( $Q$  vs  $E_{acc}$  and  $Q$  vs  $T$  at  $E_{acc} \approx 1.07$  MV/m) (see Table 2). There seems to be a correlation between the cooling rates, the flux change observed at transition by our sensor, and the cavity performance. After a new stripping, the substrate was electropolished, aiming at complete removal of the damage layer and minimal roughness. The HiPIMS coating was then applied again, following exactly the same recipe. The third coating was named BM1.3. The results, displayed in Fig. 3, evidenced a dramatic improvement of the RF performance, due to the suppression of the residual resistance (see Table 1). The Q slopes were also mitigated, and again the cavity was sensitive to the cool down conditions, indicating that a substantial component of the residual resistance was of magnetic origin.

### Substrate L1

The  $Q_0$  as function of  $E_{acc}$  for the coatings applied on the seamless substrate produced by electroforming (L1) is shown in Fig. 4, both at 4.2 K and 1.85 K.

L1 was first treated with a SUBU [23], followed by a high pressure water rinsing (HPWR) at 100 bar. Then, the Nb coating was applied via HiPIMS deposition exactly in the same way as it was done in BM1, finishing with another HPWR at 50 bar. This version was named L1.1a. The  $Q_0$  scan as a function of temperature was performed at a fixed field of  $E_{acc} \approx 0.94$  MV/m (before the Q-switch). The fitted parameters are summarized in Table 4.

As shown in Fig. 4, a Q-switch appeared at  $E_{acc} \approx 1.5$  MV/m at  $T = 4.2$  K, and at  $E_{acc} \approx 1.7$  MV/m at

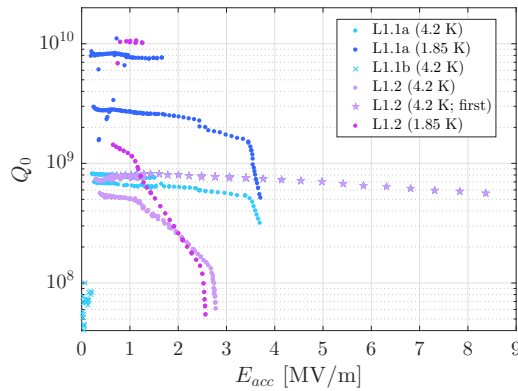


Figure 4: Quality factor ( $Q_0$ ) vs accelerating field ( $E_{acc}$ ) of the tested L1 coatings at normal and superfluid LHe.

$T = 1.85$  K. In both cases, the test was limited by field emission at  $E_{acc} \approx 3.5$  MV/m. This suggested the presence of a defect or inclusions. Hence, another HPWR at higher pressure (100 bar) was performed, aiming at getting rid of possible sources of field emission such as particulate contamination. This version was labelled as L1.1b. By comparing the  $Q_0$  measurements to L1.1a in Fig. 4, it is clear that the performance was degraded, with the  $Q_0$  rapidly decaying at low field. It was not even possible to perform a scan at 1.85 K. After the RF test, the optical inspection confirmed the presence of massive peel-off at the cut-off and the cell too. The hypothesis is that the defect in L1.1a consisted of a small peel-off which was enlarged by the HPWR.

Then, the coating was stripped and a sulfo-chromic acid rinsing was applied for passivation, aiming at improving the adherence of the coating to the substrate. This was named L1.2. It is important to highlight the good RF performance obtained in the first scan performed at  $T = 4.2$  K shown in Fig. 4. The  $Q$ -slope is very low up to  $E_{acc} \approx 9$  MV/m, where the  $Q_0$  was  $\approx 6e8$ . At that point, when the input power was increased, the  $Q_0$  suddenly dropped to  $Q_0 \approx 6e7$  and  $E_{acc} \approx 2.8$  MV/m. After that, it was not possible to reproduce that curve again and the operation was limited up to that field. Indeed, there was a  $Q$ -switch at  $E_{acc} \approx 1.3$  MV/m in both normal and superfluid tests limiting the performance of the cavity. The test was stopped at a predefined level of input power to avoid damage of the RF components. The fact of not being able to reproduce the first curve up to 9 MV/m again might be explained by the presence of a small region not well attached to the coating that, when reaching high fields, could have induced the formation of a blister or peel-off. Indeed, a blister was identified in the cell during the optical inspection after the test. A scan of  $Q_0$  vs  $T$  at  $E_{acc} \approx 0.87$  MV/m (before the  $Q$ -switch) was also performed. The obtained best fitting parameters are summarized in Table 4.

## DISCUSSION

The results of the seamless substrate BM1 with the coating applied on the surface as machined and with the damage layer partially removed (BM1.1 and BM1.2 respectively, see

Table 4: SRF Parameters of Tested L1 Coatings

	L1.1a	L1.2
$R_{res}$	33.27 n $\Omega$	23.90 n $\Omega$
$\lambda(0)$	51.54 nm	56.80 nm
$T_c$	9.362 K	9.341 K
$A_{BCS}$	1.399e5 n $\Omega$ ·K	1.682e5 n $\Omega$ ·K
$\Delta(0)/k_B$	19.76 K	19.80 K

Fig. 3), highlight once again the influence of the substrate surface state on the RF performance of the coating. More specifically, the residual resistance at low field was significantly affected (see Table 1).

Although the performance of BM1.2 was clearly improved by applying the SUBU, it still has a remarkable  $Q$  slope at 1.85 K. This might be attributed to the presence of a marbled-like pattern, found on the substrate after the chemical polishing. After removing these patterns by electropolishing, the RF performance improved dramatically. The residual resistance was reduced to a few n $\Omega$ , and the  $Q$  slope was substantially mitigated. The BM1.3 cavity was limited to 15 MV/m by a small amount of radiation, possibly due to multipacting, which is sufficient to trigger the radiation interlock at the CERN cryolab. It is now planned to test this cavity at the SM18, where RF processing will be possible.

Regarding the L1 tests, they confirm the importance of having a good adhesion of the coating to the substrate. This was obvious from the history of L1.2, whose performance was spoiled by the large delamination which occurred in two steps, corroborating the hypothesis suggested in [8] about the bad adherence being a source of  $Q$  slope.

It is worth to comment that during the tests, when reaching the power at which the  $Q$  switch occurred, two different things could happen: if the power was decreased, the  $Q$  did not recover to the curve before the switch, and hysteresis was observed. However, if the power was turned off for sufficient time, when switching it on again, the  $Q$  returned to the values before the switch (upper branch). However, for powers higher than the one triggering the switch, the  $Q$  never recovered in any case, not even turning off the power. This might be explained by a normal conducting region being activated at a certain power and sustained locally in the coating, without inducing a thermal runaway due to the high thermal diffusivity of the underlying copper.

## CONCLUSIONS

We presented the first results of Nb coatings of two seamless 1.3 GHz cavities manufactured at CERN with two different approaches: Electroformed (L1) and machined directly from a bulk billet (BM1). The RF performance shows that the  $Q$  slope has been mitigated in both cases at 4.2 K. The performance of BM1 improved significantly after removing the damaged layer present due to the machining. The third coating BM1.3, done after electropolishing the substrate, displayed a spectacular RF performance, comparable with state of the art bulk Nb, at least in the range of fields which could be explored in the small lab. We also observed a varia-

tion of the performance with thermal cycling, and a possible correlation to the flux trapping will be further studied in future tests. Regarding L1, efforts were made on improving the adherence of the coating, but peel-offs have appeared systematically. Nevertheless, results are encouraging. In particular, having removed the unknown of the weld quality, will allow a systematic work to optimise the substrate preparation and the coating parameters. The wealth of physics insight that was gathered recently with dirty Nb systems should guide this effort.

## ACKNOWLEDGEMENTS

The authors would like to thank G. Pechaud, J. Bastard, A. Gogez and S. Forel for the technical support with the preparation of the cavities and measurement setup, A. Vacca, T. Koettig, S. Prunet and L. Dufay-Chanat for providing the cryogenic infrastructure and technical help.

## REFERENCES

- [1] C. Benvenuti, N. Circelli, and M. Hauer, "Niobium films for superconducting accelerating cavities", *Appl. Phys. Lett.*, vol. 45, p. 583, 1984. doi:10.1063/1.95289
- [2] F. Gerigk, "Superconducting RF at CERN: Operation, Projects, and R&D", *IEEE Trans. Appl. Supercond.*, vol. 28, pp. 1-5, June 2018. doi:10.1109/TASC.2018.2792528
- [3] S. Aull, O. Brunner, A. Butterworth, and N. Schwerg, "Material options for the superconducting RF system of the Future Circular Collider", CERN, Geneva, Switzerland, Rep. CERN-ACC-2018-0019, April 2017.
- [4] C. Benvenuti *et al.*, "Study of the surface resistance of superconducting niobium films at 1.5 GHz", *Physica C: Superconductivity*, vol. 316, pp. 153-188, 1999. doi:10.1016/S0921-4534(99)00207-5
- [5] V. Palmieri, "RF losses due to incomplete Meissner-Ochsenfeld effect: difference between bulk Nb and Nb/Cu", presented at *TFSRF2010*, Legnaro, Italy, 2010.
- [6] S. Aull *et al.*, "On the understanding of Q-slope of niobium thin films", in *Proc. SRF'15*, Whistler, Canada, Sept. 2015. doi:10.18429/JACoW-SRF2015-TUBA03
- [7] S. Calatroni *et al.*, "Progress of Nb/Cu technology with 1.5 GHz cavities", CERN, Geneva, Switzerland, Rep. CERN-TS-2004-002, August 2014.
- [8] V. Palmieri and R. Vaglio, "Thermal contact resistance at the Nb/Cu interface as a limiting factor for sputtered thin film RF superconducting cavities", *Supercond. Sci. Technol.*, vol. 29, pp. 015004, 2015. doi:10.1088/0953-2048/29/1/015004
- [9] L. Vega, W. Venturini, G. Vandoni, and G. Rosaz, "HiPIMS from QPR to 1.3 GHz cavities", presented at *TTC2020*, CERN, Switzerland, February 2020, unpublished.
- [10] G. Rosaz *et al.*, "Biased HiPIMS technology for superconducting RF accelerating cavities coating", in *6th International*

*Conference on Fundamentals and Industrial Applications of HIPIMS 2015*, Braunschweig, Germany, June 2015.

- [11] F. Avino *et al.*, "Improved film density for coatings at grazing angle of incidence in high power impulse magnetron sputtering with positive pulse", *Thin Solid Films*, vol. 706, p. 138058, 2020. doi:10.1016/j.tsf.2020.138058
- [12] S. Calatroni *et al.*, "Performance analysis of superconducting RF cavities for the CERN rare isotope accelerator", *Phys. Rev. Accel. Beams*, vol. 19, p. 092002, 2016. doi:10.1103/PhysRevAccelBeams.19.092002
- [13] S. Teixeira Lopez *et al.*, "A Seamless Quarter-wave Resonator for HIE-ISOLDE", in *Proc. SRF'17*, Lanzhou, China, Jul. 2017, pp. 686-691. doi:10.18429/JACoW-SRF2017-WEYA03
- [14] A. Miyazaki and W. Venturini Delsolaro, "Two different origins of the Q-slope problem in superconducting niobium film cavities for a heavy ion accelerator at CERN", *Phys. Rev. Accel. Beams*, vol. 22, p. 073101, Jul. 2019. doi:10.1103/PhysRevAccelBeams.22.073101
- [15] W. Venturini Delsolaro and A. Miyazaki, "Seamless Quarter Wave Resonators for HIE ISOLDE", in *Proc. LINAC'18*, Beijing, China, Sept. 2018. doi:10.18429/JACoW-LINAC2018-TU1A05
- [16] V. Palmieri, "Metal forming technology for the fabrication of seamless superconducting radiofrequency cavities for particle accelerators", *MATEC Web of Conferences*, vol. 21, p. 04015, 2015. doi:10.1051/mateconf/20152104015
- [17] W. Singer, X. Singer, I. Jelezov, and Peter Kneisel, "Hydroforming of elliptical cavities", *Phys. Rev. Spec. Top. Accel. Beams*, vol. 18, p. 022001, 2015. doi:10.1103/PhysRevSTAB.18.022001
- [18] K. Scibor, S. Atieh, P. Trubacova, M. Gonzalez, and P. Richerot, "Machining of bulk 1.3 GHz cavity", in *Proc. eu-spen's 20th International Conference & Exhibition*, Geneva, Switzerland, Jun. 2020.
- [19] L. Lain Amador, "Production of ultra-high-vacuum chambers with integrated getter thin-film coatings by electroforming", Ph.D. thesis, U. Bourgogne Franche-Comte, Besancon, France, May 2019.
- [20] L. Lain Amador *et al.*, "Electrodeposition of copper applied to the manufacture of seamless SRF cavities", presented at *TFSRF'21*, Virtual Edition, March 2021, unpublished.
- [21] G.J. Rosaz *et al.*, "Electrodeposition of copper applied to the manufacture of seamless SRF cavities", presented at *SRF'19*, Dresden, Germany, Jul. 2019, unpublished.
- [22] H. Padamsee, J. Knobloch, and T. Hays, "Cavity testing", in *RF Superconductivity for Accelerators, 2nd Edition*, Wiley-VCH, 2008.
- [23] A. Perez Rodriguez, L. Marques Antunes Ferreira, and A. Sublet, "SUBU Characterisation: Bath Fluid Dynamics and Etching Rate", in *Proc. SRF'17*, China, 2007, pp. 575-579. doi:10.18429/JACoW-SRF2017-TUPB078